University of Nebraska - Lincoln
DigitalCommons@University of Nebraska - Lincoln

Faculty Publications -- Chemistry Department | Published Research - Department of Chemistry

1-1-2009

Quantum mechanical/molecular mechanical/continuum style solvation model: Linear response theory, variational treatment, and nuclear gradients

Hui Li
University of Nebraska - Lincoln, hli4@unl.edu

Follow this and additional works at: http://digitalcommons.unl.edu/chemfacpub

Part of the Chemistry Commons

Li, Hui, "Quantum mechanical/molecular mechanical/continuum style solvation model: Linear response theory, variational treatment, and nuclear gradients" (2009). *Faculty Publications -- Chemistry Department*. Paper 32.
http://digitalcommons.unl.edu/chemfacpub/32

This Article is brought to you for free and open access by the Published Research - Department of Chemistry at DigitalCommons@University of Nebraska - Lincoln. It has been accepted for inclusion in Faculty Publications -- Chemistry Department by an authorized administrator of DigitalCommons@University of Nebraska - Lincoln.

Quantum mechanical/molecular mechanical/continuum style solvation model: Linear response theory, variational treatment, and nuclear gradients

Hui Li[a)]
Department of Chemistry, University of Nebraska-Lincoln, Lincoln, Nebraska 68588, USA

(Received 7 August 2009; accepted 18 October 2009; published online 10 November 2009)

Linear response and variational treatment are formulated for Hartree–Fock (HF) and Kohn–Sham density functional theory (DFT) methods and combined discrete-continuum solvation models that incorporate self-consistently induced dipoles and charges. Due to the variational treatment, analytic nuclear gradients can be evaluated efficiently for these discrete and continuum solvation models. The forces and torques on the induced point dipoles and point charges can be evaluated using simple electrostatic formulas as for permanent point dipoles and point charges, in accordance with the electrostatic nature of these methods. Implementation and tests using the effective fragment potential (EFP, a polarizable force field) method and the conductorlike polarizable continuum model (CPCM) show that the nuclear gradients are as accurate as those in the gas phase HF and DFT methods. Using B3LYP/EFP/CPCM and time-dependent-B3LYP/EFP/CPCM methods, acetone $S_0 \rightarrow S_1$ excitation in aqueous solution is studied. The results are close to those from full B3LYP/CPCM calculations. © *2009 American Institute of Physics*. [doi:10.1063/1.3259550]

I. INTRODUCTION

Environmental effect plays an important role in determining molecular structures and properties in condensed phases and, therefore, must be considered in relevant quantum mechanical (QM) studies. Since full QM treatment of solvent molecules is unfeasible, efficient molecular mechanical (MM) discrete solvation models and dielectric continuum solvation models are commonly employed for this purpose. The advantages and disadvantages of these solvation models are well known. Discrete models can provide specific intermolecular interactions but usually require time-consuming simulation processes. On the other hand, continuum models are very efficient but lack of specific solute-solvent interactions and are usually very sensitive to the selection of parameters such as atomic radii. In many cases, a QM/MM/continuum style "combined discrete-continuum solvation model" is desirable.[1–5]

How to rigorously incorporate polarizable force field with induced dipoles[6] into a QM/MM/continuum style solvation model is an unsolved issue. In the combined Hartree–Fock (HF), effective fragment potential, and polarizable continuum model (HF/EFP/PCM) method developed by Bandyopadhyay, Gordon, Mennucci, and Tomasi[4] and Li, Pomelli, and Jensen,[5] linear response theory was not used to treat the self-consistently induced dipoles and charges, and a rigorous variational HF/EFP/PCM method was not formulated. Although in a later work[3] Li and Gordon realized that the linear response theory must be used for self-consistently induced dipoles and charges in the combined EFP/PCM method, a rigorous variational treatment for HF/EFP/PCM was not formulated.

Variational HF and Kohn–Sham density functional theory (DFT) methods are of fundamental importance in quantum chemistry. Many benefits can be gain by using variational HF and DFT methods. For example, analytic gradients and some other properties can be evaluated efficiently, and post-HF methods can be formulated. Therefore, it is important to incorporate solvation models into HF and DFT methods in a variational manner.

In this work a theory for variationally incorporating self-consistently induced dipole and charges into HF and DFT methods was established, and the HF/EFP/CPCM and DFT/EFP/CPCM methods were rigorously formulated and implemented. Consequently, analytic gradients for HF/EFP/CPCM and DFT/EFP/CPCM were derived and implemented. The theory is general and can be readily extended to other discrete models and continuum models.

II. THEORY

A. EFP polarization

There are two versions of the EFP method: the specific EFP method for H_2O (i.e., EFP1) and the generalized EFP method (i.e., EFP2) for any molecules.[7] Two types of fixed interactions are parameterized in the EFP1 method: electrostatic and repulsion.[8,9] Four types of fixed interactions are included in the EFP2 method: electrostatic,[10] repulsion,[11,12] charge transfer,[13] and dispersion.[14] In both EFP1 and EFP2 the intermolecular electrostatic interaction is modeled with electrostatic multipoles located at atoms and bond centers, and the polarization energy is modeled with dipole polarizability tensors located at the centroids of localized molecular orbitals of the molecules.

[a)]Author to whom correspondence should be addressed. Electronic mail: hli4@unl.edu.

 © 2009 American Institute of Physics

In the electrostatic fields ($\mathbf{F}$) created by the QM nuclei ($\mathbf{F}^{\text{nuc}}$), electrons ($\mathbf{F}^{\text{ele}}$), and multipoles of other EFPs ($\mathbf{F}^{\text{mul}}$),

$$\mathbf{F} = \mathbf{F}^{\text{nuc}} + \mathbf{F}^{\text{ele}} + \mathbf{F}^{\text{mul}}, \tag{1}$$

the polarizability tensors generate induced dipoles in a self-consistent manner. The induced dipoles, written as a column vector $\mathbf{d}$, satisfy the following *linear response* equation:

$$\mathbf{D} \cdot \mathbf{d} = \mathbf{F}. \tag{2}$$

The elements of the matrix $\mathbf{D}$ are the inverse of the nine-component dipole-dipole polarizability tensors and the Cartesian coordinates of the polarizability points. A detail description of the $\mathbf{D}$ matrix can be found in Ref. 15. Note that in Eq. (1) the electrostatic field due to EFP induced dipoles is not included; instead, it is implicitly included in the $\mathbf{D}$ matrix.

According to the linear response theory, the polarization free energy of the induced dipoles in the external field is

$$E_{\text{pol}} = -\tfrac{1}{2}\mathbf{F}^T\mathbf{d}. \tag{3}$$

The superscript "T" denotes "transpose" here and hereafter.

EFP can be used as a pure MM method with no QM part. If so, the nuclear and electronic contributions in Eq. (1) are zero, and the EFP induced dipoles are caused solely by the EFP fixed multipoles. The energy gradients (forces and torques) for all EFP-EFP interactions, including the polarization energy, have been derived and implemented.[8,10,12–15] When switching functions and periodic boundary conditions are applied, molecular dynamics (MD) simulations can be performed with EFP.[15]

The QM/MM style EFP method was first developed for HF calculations and then extended to DFT [B3LYP (Ref. 16)] method.[8,9] Detailed descriptions of the HF/EFP implementation can be found in the first paper by Day *et al.*[8] However, it is noted that approximations were used in the original implementation of the HF/EFP and DFT/EFP methods to treat the EFP asymmetric polarizabilities, and only approximate gradients were available. In this work, the rigorous variational formulas were derived and implemented, and exact gradients were obtained.

In HF/EFP and DFT/EFP calculations, both the EFP fixed interaction E_{fix} and polarization interaction E_{pol} are included in the total energy expression

$$\begin{aligned} E_{\text{total}} &= E_{\text{gas}} + E_{\text{fix}} + E_{\text{pol}} \\ &= \sum_{\mu\nu} P_{\mu\nu} h_{\mu\nu} + \frac{1}{2}\sum_{\mu\nu\rho\sigma} P_{\mu\nu}P_{\rho\sigma}\langle\mu\nu|\rho\sigma\rangle + \sum_{\mu\nu} P_{\mu\nu} V^{\text{XC}}_{\mu\nu} \\ &\quad + E_{NN} - \sum_{\mu\nu} P_{\mu\nu} V^{\text{fix}}_{\mu\nu} + E_{N,\text{fix}} + E_{\text{fix,fix}} \\ &\quad - \frac{1}{2}\sum_{\mu\nu} P_{\mu\nu} V^{\text{pol}}_{\mu\nu} + E_{N,\text{pol}} + E_{\text{fix,pol}}, \end{aligned} \tag{4}$$

where μ, ν, ρ, and σ denote basis functions, $\mathbf{P}$ is the one-particle density matrix, $\mathbf{h}_{\mu\nu}$ are one-electron integrals, $\mathbf{V}^{\text{XC}}$ is the HF exchange or the DFT exchange-correlation potential acting on the electrons, E_{NN} is the nuclear repulsion energy, $\mathbf{V}^{\text{fix}}$ is the EFP fixed potential acting on the electrons, $\mathbf{V}^{\text{pol}}$ is the EFP induced dipole potential acting on the electrons, and $E_{N,\text{fix}}$, $E_{\text{fix,fix}}$, $E_{N,\text{pol}}$, and $E_{\text{fix,pol}}$ are the interaction energies between nuclei and EFP fixed potential, between different EFP fixed potentials, between nuclei and EFP induced dipoles, and between EFP fixed potentials and induced dipoles.

Variational treatment of E_{gas} in Eq. (4) leads to the gas phase Fock or Kohn–Sham operators. Variational treatment of E_{fix} and E_{pol} leads to the following EFP operators that shall be added to the gas phase Fock or Kohn–Sham operators in the self-consistent field (SCF) calculation:

$$\mathbf{V}^{\text{fix}} + \mathbf{V}^{\text{pol}}, \tag{5}$$

where $\mathbf{V}^{\text{fix}}$ represents the effective electrostatic potential created by the EFP1 fixed terms (i.e., multipole points and repulsion points) and $\mathbf{V}^{\text{pol}}$ represents the electrostatic potential created by the induced point dipoles $\mathbf{d}$ at the electronic coordinates as if they were permanent point dipoles.

If the $\mathbf{D}$ matrix is asymmetric due to the use of asymmetric polarizability tensors, the EFP operators should be

$$\mathbf{V}^{\text{fix}} + \tfrac{1}{2}(\mathbf{V}^{\text{pol}} + \tilde{\mathbf{V}}^{\text{pol}}), \tag{6}$$

where $\tilde{\mathbf{V}}^{\text{pol}}$ represents the electrostatic potential created by another set of induced dipoles $\tilde{\mathbf{d}}$, which satisfies

$$\mathbf{D}^T \cdot \tilde{\mathbf{d}} = \mathbf{F}. \tag{7}$$

Differentiation of Eq. (4) with respect to a nuclear coordinate x produces the gradient

$$\begin{aligned} E^x_{\text{total}} &= E^x_{\text{gas}} + E^x_{\text{fix}} + E^x_{\text{pol}} \\ &= \sum_{\mu\nu} P_{\mu\nu} h^x_{\mu\nu} + \frac{1}{2}\sum_{\mu\nu\rho\sigma} P_{\mu\nu}P_{\rho\sigma}\langle\mu\nu|\rho\sigma\rangle^x + \sum_{\mu\nu} P_{\mu\nu}(V^{\text{XC}}_{\mu\nu})^x \\ &\quad + E^x_{NN} - \sum_{\mu\nu} W_{\mu\nu} S^x_{\mu\nu} - \sum_{\mu\nu} P_{\mu\nu}(V^{\text{fix}}_{\mu\nu})^x + E^x_{N,\text{fix}} + E^x_{\text{fix,fix}} \\ &\quad - (\mathbf{F}^x)^T\mathbf{d} + \frac{1}{2}\mathbf{d}^T\mathbf{D}^x\mathbf{d}, \end{aligned} \tag{8}$$

where $\mathbf{P}$ and $\mathbf{W}$ are the density matrix and energy-weighted density matrix, respectively, but both being perturbed by EFP. $\mathbf{S}$ is the basis function overlap matrix. Clearly, the explicit evaluation of the density matrix derivatives can be avoided, as originally derived by Pulay for the gas phase HF methods.[17] The derivative of the field $\mathbf{F}^x$ in Eq. (8) includes the contribution of the electronic field, which shall be evaluated with the corresponding derivatives of the basis set integrals and the density matrix $\mathbf{P}$ because all $\mathbf{P}$-dependent terms are absorbed by the energy-weighted density matrix term.

The second last term in Eq. (8) represents the forces and torques acting on the induced dipoles by the electrostatic field gradient created by the QM nuclei and electrons and EFP fixed multipoles; the last term in Eq. (8) represents the forces and torques acting on the induced dipoles by the field gradient created by other induced dipoles. If the $\mathbf{D}$ matrix is asymmetric, the last two terms in Eq. (8) should be

$$E_{\text{pol}}^{x} = -\tfrac{1}{2}(\mathbf{F}^{x})^{T}(\tilde{\mathbf{d}} + \mathbf{d}) + \tfrac{1}{2}\tilde{\mathbf{d}}^{T}\mathbf{D}^{x}\mathbf{d}. \tag{9}$$

B. Conductorlike PCM

The dielectric polarizable continuum model (DPCM),[18] integral-equation-formalism PCM (IEFPCM),[19] conductorlike PCM (CPCM),[20,21] conductorlike screening models (COSMOs),[22] generalized COSMO,[23] surface and simulation of volume polarization for electrostatics model,[24] and the SM*x* models[25] are popular quantum chemical continuum solvation models. COSMO was originally developed by Klamt and Schüürmann,[22] and CPCM (Refs. 20 and 21) is a variant of COSMO implemented in the frame of the more general IEFPCM method. Although previous studies[20,26] demonstrated that acceptable results could be obtained with COSMO and CPCM for rather low dielectric solvents, it is important to note that both COSMO and CPCM are approximations of IEFPCM, which is more accurate from an electrostatic interaction point of view, and can be used with equal accuracy for both high and low dielectric solvents.[19,27] In this work, CPCM is considered because its simplicity allows for an easier treatment in the development of analytic gradients.

CPCM describes the solvent reaction field with induced surface charges distributed on the solute cavity surface. By using boundary element method, the continuous distribution of the induced surface charge is represented by a set of induced point charges located at the surface tesserae. The CPCM induced point charges, written as a vector $\mathbf{q}$, satisfy the following linear response equation:

$$\mathbf{C}\cdot\mathbf{q} = -k\mathbf{V}, \tag{10}$$

where the elements of the symmetric matrix $\mathbf{C}$ are

$$\mathbf{C}_{ii} = 1.07\sqrt{4\pi/a_i}, \quad \mathbf{C}_{ij} = 1/|\mathbf{r}_i - \mathbf{r}_j|, \tag{11}$$

with a_i being the area and $\boldsymbol{r}_i$ being the center coordinates of tessera i.

The electrostatic potential $\mathbf{V}$ is created by the QM nuclei and electrons,

$$\mathbf{V} = \mathbf{V}^{\text{nuc}} + \mathbf{V}^{\text{ele}}. \tag{12}$$

For homogeneous solvents k in Eq. (10) is a pure number,

$$k = (\varepsilon - 1)/\varepsilon, \tag{13}$$

with ε being the dielectric constant of the solvent. Other values for k have been used in the literature. For example, Klamt and Schüürmann originally suggested $k=(\varepsilon-1)/(\varepsilon+0.5)$ for COSMO.[22] In heterogeneous IEFPCM and CPCM methods,[28] ε can be different at different regions of the solute surface, and k should be replaced by a diagonal matrix $\mathbf{K}$.

According to the linear response theory, the CPCM solvation free energy due to induced surface charge is

$$E_{\text{sol}} = \tfrac{1}{2}\mathbf{V}^{T}\mathbf{q}. \tag{14}$$

The electrostatic potential generated by the induced surface charges can be incorporated into the HF and Kohn–Sham equations to variationally determine the total molecular energy E_{total} using a finite basis set,

$$\begin{aligned} E_{\text{total}} &= E_{\text{gas}} + E_{\text{sol}} \\ &= \sum_{\mu\nu} P_{\mu\nu}h_{\mu\nu} + \frac{1}{2}\sum_{\mu\nu\rho\sigma} P_{\mu\nu}P_{\rho\sigma}\langle\mu\nu|\rho\sigma\rangle + \sum_{\mu\nu} P_{\mu\nu}V_{\mu\nu}^{\text{XC}} \\ &\quad + E_{NN} - \frac{1}{2}\sum_{\mu\nu} P_{\mu\nu}V_{\mu\nu}^{\text{sol}} + E_{N,\text{sol}}, \end{aligned} \tag{15}$$

where $\mathbf{V}^{\text{sol}}$ is the CPCM induced charge potential acting on the electrons and $E_{N,\text{sol}}$ is the interaction energy between QM nuclei and CPCM induced charges.

Variational treatment of Eq. (15) leads to the gas phase Fock or Kohn–Sham operators, as well as a CPCM solvation operator that shall be added to the gas phase Fock or Kohn–Sham operators in the SCF calculation,

$$\mathbf{V}^{\text{sol}} = \sum_{i} \mathbf{q}_i/|\mathbf{r}_e - \mathbf{r}_i|, \tag{16}$$

where $\mathbf{q}_i$ is the CPCM induced charge at tessera i, $\mathbf{r}_i$ is the coordinate of tessera i, $\mathbf{r}_e$ is the electronic coordinate, and i runs over all surface tesserae. Clearly, $\mathbf{V}^{\text{sol}}$ is evaluated as if the induced charges were permanent point charges.

If the $\mathbf{C}$ matrix is asymmetric, such as in DPCM and IEFPCM, or due to the introduction of heterogeneity, the PCM operators should be

$$\tfrac{1}{2}(\mathbf{V}^{\text{sol}} + \tilde{\mathbf{V}}^{\text{sol}}) \tag{17}$$

where $\tilde{\mathbf{V}}^{\text{sol}}$ represents the electrostatic potential created by another set of induced charges $\tilde{\mathbf{q}}$, which satisfies

$$\mathbf{C}^{T}\cdot\tilde{\mathbf{q}} = -k\mathbf{V}. \tag{18}$$

Differentiation of Eq. (15) with respect to a nuclear coordinate x produces the gradient

$$\begin{aligned} E_{\text{total}}^{x} &= E_{\text{gas}}^{x} + E_{\text{sol}}^{x} \\ &= \sum_{\mu\nu} P_{\mu\nu}h_{\mu\nu}^{x} + \frac{1}{2}\sum_{\mu\nu\rho\sigma} P_{\mu\nu}P_{\rho\sigma}\langle\mu\nu|\rho\sigma\rangle^{x} \\ &\quad + \sum_{\mu\nu} P_{\mu\nu}(V_{\mu\nu}^{\text{XC}})^{x} + E_{NN}^{x} - \sum_{\mu\nu} W_{\mu\nu}S_{\mu\nu}^{x} + (\mathbf{V}^{x})^{T}\mathbf{q} \\ &\quad - \frac{1}{2}k^{-1}\mathbf{q}^{T}\mathbf{C}^{x}\mathbf{q}, \end{aligned} \tag{19}$$

where $\mathbf{P}$ and $\mathbf{W}$ are the density matrix and energy-weighted density matrix, respectively, but both perturbed by CPCM. Again, the explicit evaluation of the density matrix derivatives can be avoided. The derivative of the potential $\mathbf{V}^{x}$ in Eq. (19) includes the contribution of the electrons, which shall be evaluated with the corresponding derivatives of the basis set integrals and the density matrix $\mathbf{P}$ because all $\mathbf{P}$-dependent terms are absorbed by the energy-weighted density matrix term.

The second last term in Eq. (19) represents the forces acting on the induced charges by the electrostatic field created by the nuclei and electrons of the QM molecule and EFP fixed multipoles; the last term in Eq. (19) represents the forces between the induced charges. If the $\mathbf{C}$ matrix is asymmetric, the last two terms in Eq. (19) should be

$$E_{\mathrm{sol}}^{x} = +\tfrac{1}{2}(\mathbf{V}^{x})^{T}(\tilde{\mathbf{q}}+\mathbf{q}) - \tfrac{1}{2}k^{-1}\tilde{\mathbf{q}}^{T}\mathbf{C}^{x}\mathbf{q}. \tag{20}$$

CPCM has been implemented for restricted Hartree-Fock (RHF), restricted open-shell Hartree-Fock (ROHF), unrestricted Hartree-Fock (UHF), and multiconfiguration self-consistent field (MCSCF) wave functions[29] and has been interfaced with the fragment molecular orbital method.[30] Using a recently developed tessellation scheme called fixed points with variable areas (FIXPVA), smooth CPCM potential energy surfaces and accurate analytic gradients have been obtained for RHF, ROHF, UHF methods and their DFT analogs, and the MCSCF methods.[31]

C. DFT/EFP/CPCM and HF/EFP/CPCM

Because the EFP induced dipoles and CPCM induced charges satisfy linear response equations [i.e., Eqs. (2) and (10)], they must satisfy similar linear response equations in combined EFP/CPCM calculations. In the earlier HF/EFP/PCM implementation linear response theory was not used to treat the induced dipoles charges and a rigorous variational HF/EFP/PCM method was not formulated.[4,5]

Li and Gordon[3] developed a linear response "supermatrix equation" to link the self-consistently induced dipoles and charges to the electrostatic fields and potentials created by QM nuclei, QM electrons, and EFP multipole points,

$$\mathbf{B}\cdot\mathbf{w} = \mathbf{P}. \tag{21}$$

It is named as a supermatrix equation because $\mathbf{P}$ is a combined set of the electrostatic fields ($\mathbf{F}$) at the polarizability points and the negative electrostatic potentials ($\mathbf{V}$, corrected by k) at the CPCM tesserae due to QM molecules and EFP fixed static multipoles (note that the field due to CPCM charges and the potential due to EFP induced dipoles are excluded); $\mathbf{w}$ is a combined set of induced dipoles ($\mathbf{d}$) and induced charges ($\mathbf{q}$),

$$\mathbf{P} = \begin{pmatrix} \mathbf{F} \\ -k\mathbf{V} \end{pmatrix}, \quad \mathbf{w} = \begin{pmatrix} \mathbf{d} \\ \mathbf{q} \end{pmatrix}. \tag{22}$$

$\mathbf{B}$ is a geometric matrix, which can be written in block form as

$$\mathbf{B} = \begin{pmatrix} \mathbf{D} & \mathbf{R} \\ \mathbf{R}^{T} & \mathbf{C} \end{pmatrix}. \tag{23}$$

The $\mathbf{D}$ and $\mathbf{C}$ blocks are exactly the $\mathbf{D}$ and $\mathbf{C}$ matrices in Eqs. (2) and (10), respectively. The matrix $\mathbf{R}$ is a matrix operator that acts on the CPCM induced charges to produce negative electrostatic fields at the EFP polarizability points. $\mathbf{R}^{T}$ is the transpose of $\mathbf{R}$ and serves as a matrix operator that acts on the EFP induced dipoles to produce electrostatic potentials at the CPCM tesserae.

The physical meaning of the supermatrix Eq. (21) is that the EFP induced dipoles and CPCM induced charges are uniquely determined by the field and potential of the QM nuclei and electrons and the EFP static multipoles. A detailed description of the $\mathbf{D}$ matrix can be found in Ref. 3.

According to the linear response theory, the EFP/CPCM polarization free energy is

$$\begin{aligned} E_{\mathrm{pol+sol}} &= -\tfrac{1}{2}\mathbf{P}^{T}\mathbf{w} \\ &= -\tfrac{1}{2}\mathbf{F}^{T}\mathbf{d} + \tfrac{1}{2}\mathbf{V}^{T}\mathbf{q} \\ &= -\tfrac{1}{2}(\mathbf{F}^{\mathrm{nuc}} + \mathbf{F}^{\mathrm{ele}} + \mathbf{F}^{\mathrm{mul}})^{T}\mathbf{d} + \tfrac{1}{2}(\mathbf{V}^{\mathrm{nuc}} + \mathbf{V}^{\mathrm{ele}} + \mathbf{V}^{\mathrm{mul}})^{T}\mathbf{q}. \end{aligned} \tag{24}$$

Clearly, there is no explicit interaction term involving induced dipoles and induced charges because they have already been implicitly included. Equation (24) is different from the corresponding equations in Refs. 4 and 5. In both Refs. 4 and 5, the following EFP polarization energy E_{pol} and PCM polarization energy E_{sol} were defined:

$$\begin{aligned} E_{\mathrm{pol}} + E_{\mathrm{sol}} = &-\tfrac{1}{2}(\mathbf{F}^{\mathrm{nuc}} + \mathbf{F}^{\mathrm{ele}} + \mathbf{F}^{\mathrm{mul}})^{T}\mathbf{d} \\ &+ \tfrac{1}{2}(\mathbf{V}^{\mathrm{nuc}} + \mathbf{V}^{\mathrm{ele}} + \mathbf{V}^{\mathrm{mul}} + \mathbf{V}^{\mathrm{pol}})^{T}\mathbf{q}, \end{aligned} \tag{25}$$

where $\mathbf{V}^{\mathrm{pol}}$ is the electrostatic potential created by the EFP induced dipoles at the PCM surface tesserae. Compared to Eq. (24), Eq. (25) has an extra interaction term $\frac{1}{2}(\mathbf{V}^{\mathrm{pol}})^{T}\mathbf{q}$, double counting the interaction between the EFP induced dipoles and PCM induced charges. This double counting does not conform the linear response assumption made in both the EFP and PCM methods.

Although Eqs. (21)–(24) were used by Li and Gordon[3] to derive the polarization energy gradients for the EFP induced dipoles and PCM induced charges, a rigorous variational treatment was not formulated for HF/EFP/PCM and DFT/EFP/PCM methods, and the energy and gradients contain some approximations pertaining to the initial implementation of the HF/EFP method.[8] The first approximation was made in the formation of the EFP induced dipole operator to be added to the Fock operator. According to the linear response and variational treatment, the induced dipole operator is simply the electrostatic potential created by the induced dipoles at the electronic coordinates. However, in the original implementation of the HF/EFP method, a complicated but approximate operator was formed. It was found that the approximation is very accurate, producing energies and gradients that are accurate to $\sim 10^{-7}$ and $\sim 10^{-5}$ a.u., respectively. The other approximation was made to treat the asymmetric EFP polarizability tensors in gradient calculations, which also lead to $\sim 10^{-5}$ a.u. errors in the gradients. The second approximation was removed earlier.[3] The first approximation was removed in this work.

In this work, the rigorous variational HF/EFP/CPCM and DFT/EFP/CPCM methods are formulated. This starts by including the EFP fixed interactions (E_{fix}) and the EFP/CPCM polarization interactions ($E_{\mathrm{pol+sol}}$) in the DFT or HF energy expression

$$
\begin{aligned}
E_{\text{total}} &= E_{\text{gas}} + E_{\text{fix}} + E_{\text{pol+sol}} \\
&= \sum_{\mu\nu} P_{\mu\nu} h_{\mu\nu} + \frac{1}{2} \sum_{\mu\nu\rho\sigma} P_{\mu\nu} P_{\rho\sigma} \langle \mu\nu | \rho\sigma \rangle \\
&\quad + \sum_{\mu\nu} P_{\mu\nu} V_{\mu\nu}^{\text{XC}} + E_{NN} - \sum_{\mu\nu} P_{\mu\nu} V_{\mu\nu}^{\text{fix}} + E_{N,\text{fix}} + E_{\text{fix,fix}} \\
&\quad - \frac{1}{2} \sum_{\mu\nu} P_{\mu\nu} V_{\mu\nu}^{\text{pol}} + E_{N,\text{pol}} + E_{\text{fix,pol}} \\
&\quad - \frac{1}{2} \sum_{\mu\nu} P_{\mu\nu} V_{\mu\nu}^{\text{sol}} + E_{N,\text{sol}} + E_{\text{fix,sol}},
\end{aligned} \tag{26}
$$

where the notations are the same as defined before, with $E_{\text{fix,sol}}$ representing the interaction energies between EFP fixed potential and CPCM induced charges.

Variational treatment of Eq. (26) leads to the gas phase Fock or Kohn–Sham operators plus the following EFP/CPCM operators (potentials) that shall be added to the gas phase Fock or Kohn–Sham operators in SCF calculations:

$$
\mathbf{V}^{\text{fix}} + \mathbf{V}^{\text{pol}} + \mathbf{V}^{\text{sol}}. \tag{27}
$$

The potentials due to EFP induced dipoles ($\mathbf{V}^{\text{pol}}$) and CPCM induced charges ($\mathbf{V}^{\text{sol}}$) are evaluated as if they were permanent point dipoles and point charges.

If the $\mathbf{B}$ matrix is asymmetric, for example, due to the use of asymmetric $\mathbf{C}$ matrix for IEFPCM or heterogeneous CPCM or the use asymmetric and anisotropic polarizability tensors in the $\mathbf{D}$ matrix, these operators should be

$$
\mathbf{V}^{\text{fix}} + \tfrac{1}{2}(\mathbf{V}^{\text{pol}} + \tilde{\mathbf{V}}^{\text{pol}} + \mathbf{V}^{\text{sol}} + \tilde{\mathbf{V}}^{\text{sol}}), \tag{28}
$$

where $\tilde{\mathbf{V}}^{\text{pol}}$ and $\tilde{\mathbf{V}}^{\text{sol}}$ represent, respectively, the electrostatic potentials created by $\tilde{\mathbf{d}}$ and $\tilde{\mathbf{q}}$, which satisfy

$$
\mathbf{B}^T \cdot \begin{pmatrix} \tilde{\mathbf{d}} \\ \tilde{\mathbf{q}} \end{pmatrix} = \mathbf{P}. \tag{29}
$$

Differentiation of Eq. (26) with respect to a nuclear coordinate x produces the gradient

$$
\begin{aligned}
E_{\text{total}}^x &= E_{\text{gas}}^x + E_{\text{fix}}^x + E_{\text{pol+sol}}^x \\
&= \sum_{\mu\nu} P_{\mu\nu} h_{\mu\nu}^x + \frac{1}{2} \sum_{\mu\nu\rho\sigma} P_{\mu\nu} P_{\rho\sigma} \langle \mu\nu | \rho\sigma \rangle^x \\
&\quad + \sum_{\mu\nu} P_{\mu\nu} (V_{\mu\nu}^{\text{XC}})^x + E_{NN}^x - \sum_{\mu\nu} W_{\mu\nu} S_{\mu\nu}^x \\
&\quad - \sum_{\mu\nu} P_{\mu\nu} (V_{\mu\nu}^{\text{fix}})^x + E_{N,\text{fix}}^x + E_{\text{fix,fix}}^x - (\mathbf{F}^x)^T \mathbf{d} \\
&\quad + (\mathbf{V}^x)^T \mathbf{q} + \mathbf{d}^T \mathbf{R}^x \mathbf{q} + \frac{1}{2} \mathbf{d}^T \mathbf{D}^x \mathbf{d} + \frac{1}{2} k^{-1} \mathbf{q}^T \mathbf{C}^x \mathbf{q},
\end{aligned} \tag{30}
$$

where $\mathbf{P}$ and $\mathbf{W}$ are the density matrix and energy-weighted density matrix, respectively, but both being perturbed by EFP/PCM. Again, the explicit evaluation of the density matrix derivatives can be avoided, and the electronic contributions of derivative of the field $\mathbf{F}^x$ and potential $\mathbf{V}^x$ are evaluated with the corresponding derivatives of the basis set integrals and the density matrix $\mathbf{P}$ because all $\mathbf{P}$-dependent terms are absorbed by the energy-weighted density matrix term.

Four of the last five terms in Eq. (30) have the same physical meanings as those in Eqs. (8) and (19). The new term $\mathbf{d}^T \mathbf{R}^x \mathbf{q}$ represents the forces and torques between the EFP induced dipoles and CPCM induced charges. All of them can be evaluated as simple electrostatic forces and torques, in accordance with the electrostatic nature of these methods. In addition, the formulas for permanent point dipoles and charges can be used for induced point dipoles and charges as if they were permanent point dipoles and charges.

If the $\mathbf{B}$ matrix is asymmetric, the last five terms in Eq. (30) should be

$$
\begin{aligned}
E_{\text{pol+sol}}^x &= -\tfrac{1}{2}(\mathbf{F}^x)^T(\tilde{\mathbf{d}} + \mathbf{d}) + \tfrac{1}{2}(\mathbf{V}^x)^T(\tilde{\mathbf{q}} + \mathbf{q}) + \tfrac{1}{2}\tilde{\mathbf{d}}^T \mathbf{R}^x \mathbf{q} \\
&\quad + \tfrac{1}{2}\mathbf{d}^T \mathbf{R}^x \tilde{\mathbf{q}} + \tfrac{1}{2}\tilde{\mathbf{d}}^T \mathbf{D}^x \mathbf{d} + \tfrac{1}{2} k^{-1} \tilde{\mathbf{q}}^T \mathbf{C}^x \mathbf{q}.
\end{aligned} \tag{31}
$$

III. NUMERICAL RESULTS

A. Implementation

The linear response and variational DFT/EFP/CPCM, HF/EFP/CPCM, and MCSCF/EFP/CPCM methods (both energy and gradients) have been implemented in the GAMESS (Ref. 32) package based on the QM/EFP/PCM code[4,5] implemented previously. The CPCM code was previously implemented by Li and Jensen[21] on the basis of the IEFPCM program originally implemented by Mennucci, Cances, Pomelli, and Tomasi.[5,19,33] The code has been released in the January 12, 2009, version of GAMESS.

Tests show that the analytic gradients for both HF/EFP/CPCM and DFT/EFP/CPCM methods are accurate to $10^{-7} \sim 10^{-6}$ hartree/bohr or hartree/rad. Such accurate gradients are partially due to the use of the FIXPVA tessellation scheme developed by the author's group for CPCM.[31] Similarly accurate gradients have also been observed for DFT/EFP, HF/EFP, and EFP/CPCM (no QM molecule) calculations. Using such accurate gradients, QM/MM/continuum style MD simulations have been performed with good energy conservation. It must be noted that in GAMESS gradients are subject to projection that eliminates rotational gradients (torques) artificially exerted on the molecules by the DFT grid points or the PCM surface grid points (tesserae) in order to improve geometry optimization convergence. The projection can typically alter the gradients by $\sim 10^{-4}$ a.u. Therefore, to reproduce the exact gradients reported in the current paper, one needs to turn the projection off by changing the GAMESS source code in *grd2a.src*.

B. Acetone $n \rightarrow \pi^*$ transition

QM/MM/continuum style methods can be used to study electronically excited molecules in solvents. In general, solvents can affect the excitation of a molecule in three ways: (1) the solvent affects the ground state molecular and electronic structures and thus affects the vertical excitation energy, (2) the solvent affects the excitation process and thus also affects the vertical excitation energy, and (3) the solvent affects the excited molecular and electronic structures. Vari-

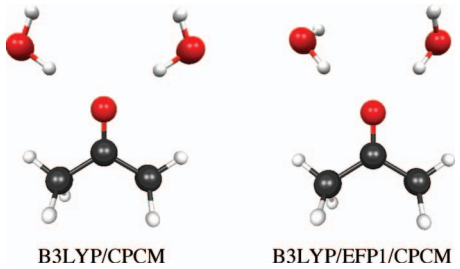

FIG. 1. Acetone and two water molecules (Ac2W) optimized in aqueous solution with B3LYP/CPCM and B3LYP/EFP1/CPCM methods.

ous QM/MM and QM/MM/continuum style methods have been developed to study excited molecules, for example, by Öhrn and Karlström,[2] Lin and Gao,[34] Kongsted, Osted, and Mikkelsen,[35] Jensen, van Duijnen, Snijders, and Netzel,[36] and Yoo, Zhariev, Sok, and Gordon.[37] However, none of these methods have included self-consistently induced dipoles and induced charges in the study of excited states.

Here a typical case, acetone $n \rightarrow \pi^*$ valence transition in the gas phase and aqueous solution, is studied with the QM/EFP/CPCM method developed in the current work. In the $n \rightarrow \pi^*$ transition an electron in the oxygen lone pair nonbonding orbital n is excited to the C=O antibonding orbital π^*. This transition has been studied experimentally and theoretically (see Aidas *et al.*[38] and references therein). An interesting phenomenon is the experimentally observed ~0.20 eV blueshift of the $S_0 \rightarrow S_1$ transition in aqueous solution, which cannot be reproduced by using continuum solvation models or nondynamic supermolecule approaches. Even with dynamic simulations, reliable results are still difficult to obtain.[38] Recently, Yoo *et al.* used QM/MM style Born–Oppenheimer *ab initio* MD simulation to determine the dynamic structures of acetone and 100 water molecules (with B3LYP and the B3LYP type EFP1 method[9]) and then successfully reproduced the average blueshift with the time-dependent(TD)-B3LYP/EFP1 method.[37]

The geometry of acetone was optimized in the gas phase and aqueous solution phase with the B3LYP and B3LYP/CPCM methods, respectively. The aug-cc-pVDZ basis set[39] was used for all the calculations. This basis set is sufficient for valence excitation calculations. The geometry of acetone and two water molecules (Fig. 1), denoted as Ac2W, was optimized in aqueous solution phase with the B3LYP/CPCM method, as well as the B3LYP/EFP1/CPCM method in which the water molecules were represented by the B3LYP type EFP1 method[9] and the bulk water was described by CPCM. No symmetry was imposed in the geometry optimization. In the B3LYP calculation 96 radial and 302 Lebedev angular grid points were used. In equilibrium CPCM calculations, $\varepsilon = 78.39$ was used. In nonequilibrium CPCM and TD-B3LYP [i.e., TD-B3LYP/CPCM (Ref. 40)] calculations, the optical $\varepsilon_\infty = 1.776$ was used for water. In the CPCM calculations, spheres with radii of 0, 2.124, 2.016, and 1.908 were used for H, C, N, and O atoms, respectively, to define the molecular cavity; no additional spheres were used. Using zero radii for H atoms means that they do not contribute to form the surface. The tessellation scheme FIXPVA was used with 60 initial tesserae per sphere.[31] The induced surface charges were determined by a semi-iterative direct inversion of the iterative subspace (DIIS) procedure[5,41] with no charge renormalization. Only the electrostatic interaction was considered; cavitation, dispersion, and repulsion terms were not considered. The optimized geometries were verified by Hessian calculations to be minimum points on the potential energy surfaces.

The gas phase B3LYP optimized C=O bond length is 1.217 Å, in good agreement with the experimental value of 1.215 Å.[42] When solvation models are included, the C=O bond length becomes slightly longer (Table I). The B3LYP/CPCM and B3LYP/EFP1/CPCM optimized Ac2W structures are slightly different (Fig. 1 and Table I). The B3LYP/CPCM one is near planar, with the distances between the O atoms being 2.862, 2.861, and 4.666 Å. The B3LYP/EFP1/CPCM one has two water hydrogen atoms sticking out of the plane, with the distances between the O atoms being 2.827, 2.829, and 3.907 Å (Table I). As will be discussed later, the structure difference is not the main cause of the difference in the calculated excitation energies.

The TD-B3LYP method[43] was used to calculate the $S_0 \rightarrow S_1$ vertical excitation energies (Table I). The result calculated with the gas phase TD-B3LYP method on the basis of the gas phase B3LYP optimized ground state geometry is 4.36 eV, in good agreement with an experimental maximum absorption value of 4.38 eV reported by Walzl, Koerting, and Kuppermann using electron scattering method.[44]

The TD-B3LYP/CPCM(equilibrium) vertical excitation energy based on the B3LYP/CPCM optimized ground state geometry is 4.48 eV, showing a blueshift of 0.12 eV as compared to the gas phase value. Considering nonequilibrium CPCM effect in the TD-B3LYP calculation, the result is 4.49 eV, very close to the equilibrium-CPCM value of 4.48 eV. Similarly small effects were seen in the random-phase-approximation results reported by Mennucci, Cammi,

TABLE I. Acetone geometric parameters (angstrom) and $S_0 \rightarrow S_1$ vertical transition energies (eV) in the gas phase and aqueous solution.

	Distances[a]				ΔE_{excite}	
	C=O	O···O1	O···O2	O1···O2	Exp.	Cal.
Acetone gas phase	1.217				4.38	4.36
Acetone+CPCM	1.227				~4.58	4.48
Acetone+2 H_2O+CPCM	1.234	2.862	2.861	4.666	~4.58	4.71
Acetone+2 EFP1+CPCM	1.230	2.827	2.829	3.907	~4.58	4.67

[a]O1=O atom of water 1 and O2=O atom of water 2.

and Tomasi.[45] Experiments show that the blueshift of the acetone $S_0 \rightarrow S_1$ transition in aqueous solution is about 0.20 eV.[46] Clearly, CPCM underestimates the blueshift due to the lacking of specific solvent interactions. This has been discussed in the literature.[38,45,47]

The TD-B3LYP/CPCM calculated blueshift based on B3LYP/CPCM optimized geometry of the Ac2W complex (Fig. 1) is 0.35 eV. Currently, a rigorous TD-B3LYP/EFP1/CPCM method is not available. Here an approximate method is used: in the ground state B3LYP/EFP1/CPCM calculation, the EFP induced dipoles and CPCM induced charges are determined self-consistently using Eq. (21), while in the linear response calculation, these dipoles and charges are included independently with no mutual interactions. Although not rigorous, it can be expected that the errors are very small. Using the approximate TD-B3LYP/EFP1/CPCM method, the blueshift for the Ac2W complex is 0.31 eV, smaller than the full B3LYP/CPCM value by 0.04 eV. The geometric difference between the B3LYP/CPCM and B3LYP/EFP1/CPCM optimized Ac2W complex is not the main cause of the 0.04 eV difference. A test TD-B3LYP/EFP1/CPCM calculation using the B3LYP/CPCM optimized Ac2W geometry actually resulted in a 0.05 eV difference. Therefore, the difference is mainly caused by the intrinsic differences in the EFP1 interactions as compared to full B3LYP method. Yoo *et al.* reported similar agreement between full B3LYP and B3LYP/EFP1 methods (no CPCM) for acetone.[37] Clearly, including explicit solvent interactions leads to more significant blueshifts, and dynamic effects should be considered in order to explain the experimental blueshift.[37] With accurate analytic gradients, B3LYP/EFP1/CPCM can be used to perform MD simulation. The results of QM/EFP/CPCM dynamic simulations will be reported in future publications.

IV. CONCLUSION

A general variational theory is established for incorporating self-consistently induced dipole and charges into HF and DFT methods and is applied to the HF/EFP/CPCM and DFT/EFP/CPCM methods. To conclude, the following points are highlighted.

(1) The induced dipoles and charges must be determined self-consistently according to the linear response theory [Eq. (21)].

(2) The electrostatic potentials acting on the electrons (i.e., polarization operators to be added into the Fock or Kohn–Sham operators) due to induced dipoles and charges must be evaluated as if they were permanent dipoles and charges. If asymmetric polarization is involved, two sets of induced dipoles and charges are required [Eqs. (28) and (29)].

(3) Analytic gradients can be evaluated efficiently in a way similar to the gas phase HF and DFT methods by using energy-weighted density matrix [Eq. (30)]. The forces and torques on the induced dipoles and charges can be evaluated as for permanent point dipoles and charges. Numerical tests show that the analytic gradients are accurate to $10^{-7}-10^{-6}$ a.u.

(4) The B3LYP/EFP1/CPCM and TD-B3LYP/EFP1/CPCM methods were used to study acetone $S_0 \rightarrow S_1$ transition, and the results are in good agreement with the corresponding full B3LYP/CPCM and TD-B3LYP/CPCM results.

(5) The theory is general and can be readily extended to other polarizable force fields and continuum models.

ACKNOWLEDGMENTS

This work was supported by start-up funds from the University of Nebraska-Lincoln.

[1] A. H. Devries, P. T. van Duijnen, A. H. Juffer, J. A. C. Rullmann, J. P. Dijkman, H. Merenga, and B. T. Thole, J. Comput. Chem. **16**, 37 (1995); P. Bandyopadhyay and M. S. Gordon, J. Chem. Phys. **113**, 1104 (2000); Q. Cui, *ibid.* **117**, 4720 (2002).
[2] A. Ohrn and G. Karlstrom, Mol. Phys. **104**, 3087 (2006).
[3] H. Li and M. S. Gordon, J. Chem. Phys. **126**, 124112 (2007).
[4] P. Bandyopadhyay, M. S. Gordon, B. Mennucci, and J. Tomasi, J. Chem. Phys. **116**, 5023 (2002).
[5] H. Li, C. S. Pomelli, and J. H. Jensen, Theor. Chem. Acc. **109**, 71 (2003).
[6] F. J. Vesely, J. Comput. Phys. **24**, 361 (1977); M. Neumann, F. J. Vesely, O. Steinhauser, and P. Schuster, Mol. Phys. **35**, 841 (1978); F. H. Stillinger and C. W. David, J. Chem. Phys. **69**, 1473 (1978); P. Barnes, J. L. Finney, J. D. Nicholas, and J. E. Quinn, Nature (London) **282**, 459 (1979); A. Warshel, J. Phys. Chem. **83**, 1640 (1979).
[7] M. S. Gordon, M. A. Freitag, P. Bandyopadhyay, J. H. Jensen, V. Kairys, and W. J. Stevens, J. Phys. Chem. A **105**, 293 (2001); M. S. Gordon, L. Slipchenko, H. Li, and J. H. Jensen, *The Effective Fragment Potential: A General Method for Predicting Intermolecular Interactions* (Elsevier, Amsterdam, 2007).
[8] P. N. Day, J. H. Jensen, M. S. Gordon, S. P. Webb, W. J. Stevens, M. Krauss, D. Garmer, H. Basch, and D. Cohen, J. Chem. Phys. **105**, 1968 (1996).
[9] I. Adamovic, M. A. Freitag, and M. S. Gordon, J. Chem. Phys. **118**, 6725 (2003).
[10] L. V. Slipchenko and M. S. Gordon, J. Comput. Chem. **28**, 276 (2007).
[11] J. H. Jensen and M. S. Gordon, Mol. Phys. **89**, 1313 (1996).
[12] H. Li and M. S. Gordon, Theor. Chem. Acc. **115**, 385 (2006).
[13] H. Li, M. S. Gordon, and J. H. Jensen, J. Chem. Phys. **124**, 214108 (2006).
[14] I. Adamovic and M. S. Gordon, Mol. Phys. **103**, 379 (2005).
[15] H. Li, H. M. Netzloff, and M. S. Gordon, J. Chem. Phys. **125**, 194103 (2006).
[16] R. H. Hertwig and W. Koch, Chem. Phys. Lett. **268**, 345 (1997); A. D. Becke, Phys. Rev. A **38**, 3098 (1988); C. Lee, W. Yang, and R. G. Parr, Phys. Rev. B **37**, 785 (1988).
[17] P. Pulay, Mol. Phys. **17**, 197 (1969).
[18] S. Mierts, E. Scrocco, and J. Tomasi, Chem. Phys. **55**, 117 (1981).
[19] E. Cances, B. Mennucci, and J. Tomasi, J. Chem. Phys. **107**, 3032 (1997).
[20] V. Barone and M. Cossi, J. Phys. Chem. A **102**, 1995 (1998).
[21] H. Li and J. H. Jensen, J. Comput. Chem. **25**, 1449 (2004).
[22] A. Klamt and G. Schuurmann, J. Chem. Soc., Perkin Trans. 2 **1993**, 799.
[23] T. N. Truong and E. V. Stefanovich, Chem. Phys. Lett. **240**, 253 (1995).
[24] D. M. Chipman, Theor. Chem. Acc. **107**, 80 (2002); D. M. Chipman and M. Dupuis, *ibid.* **107**, 90 (2002).
[25] A. V. Marenich, R. M. Olson, C. P. Kelly, C. J. Cramer, and D. G. Truhlar, J. Chem. Theory Comput. **3**, 2011 (2007).
[26] M. Cossi, N. Rega, G. Scalmani, and V. Barone, J. Comput. Chem. **24**, 669 (2003).
[27] B. Mennucci, E. Cances, and J. Tomasi, J. Phys. Chem. B **101**, 10506 (1997).
[28] M. F. Iozzi, M. Cossi, R. Improta, N. Rega, and V. Barone, J. Chem. Phys. **124**, 184103 (2006); D. Si and H. Li, *ibid.* **131**, 044123 (2009).
[29] H. Li, S. P. Webb, J. Ivanic, and J. H. Jensen, J. Am. Chem. Soc. **126**, 8010 (2004).
[30] H. Li, D. G. Fedorov, T. Nagata, K. Kitaura, J. H. Jensen, and M. S. Gordon, "Energy gradients in combined fragment molecular orbital and polarizable continuum model (FMO/PCM) calculation," J. Comput.

Chem. (published online, Juen 30, 2009).
[31] P. Su and H. Li, J. Chem. Phys. **130**, 074109 (2009).
[32] M. W. Schmidt, K. K. Baldridge, J. A. Boatz, S. T. Elbert, M. S. Gordon, J. H. Jensen, S. Koseki, N. Matsunaga, K. A. Nguyen, S. J. Su, T. L. Windus, M. Dupuis, and J. A. Montgomery, J. Comput. Chem. **14**, 1347 (1993); M. S. Gordon and M. W. Schmidt, *Advances in Electronic Structure Theory: GAMESS a Decade Later* (Elsevier, Amsterdam, 2005).
[33] J. Tomasi, B. Mennucci, and E. Cances, J. Mol. Struct.: THEOCHEM **464**, 211 (1999).
[34] I. J. Lin, E. B. Gebel, T. E. Machonkin, W. M. Westler, and J. L. Markley, Proc. Natl. Acad. Sci. U.S.A. **102**, 14581 (2005).
[35] J. Kongsted, A. Osted, K. V. Mikkelsen, and O. Christiansen, J. Chem. Phys. **118**, 1620 (2003); J. Kongsted, A. Osted, K. V. Mikkelsen, P.-O. Astrand, and O. Christiansen, *ibid.* **121**, 8435 (2004).
[36] L. Jensen, P. T. van Duijnen, and J. G. Snijders, J. Chem. Phys. **119**, 3800 (2003); P. T. Van Duijnen and T. L. Netzel, J. Phys. Chem. A **110**, 2204 (2006); C. R. Jacob, J. Neugebauer, L. Jensen, and L. Visscher, Phys. Chem. Chem. Phys. **8**, 2349 (2006).
[37] S. Yoo, F. Zahariev, S. Sok, and M. S. Gordon, J. Chem. Phys. **129**, 144112 (2008).
[38] K. Aidas, J. Kongsted, A. Osted, K. V. Mikkelsen, and O. Christiansen, J. Phys. Chem. A **109**, 8001 (2005).
[39] T. H. Dunning, J. Chem. Phys. **90**, 1007 (1989).
[40] M. Cossi and V. Barone, J. Chem. Phys. **115**, 4708 (2001).
[41] C. S. Pomelli, J. Tomasi, and V. Barone, Theor. Chem. Acc. **105**, 446 (2001).
[42] L. M. Sverdlov, M. A. Kovner, and E. P. Krainov, *Vibrational Spectra of Polyatomic Molecules* (Wiley, New York, 1974).
[43] M. E. Casida, in *Recent Advances in Density Functional Methods*, edited by D. P. Chong (World Scientific, Singapore, 1995), pp. 155; M. E. Casida, C. Jamorski, K. C. Casida, and D. R. Salahub, J. Chem. Phys. **108**, 4439 (1998); M. Chiba, T. Tsuneda, and K. Hirao, *ibid.* **124**, 141106 (2006); M. Chiba, T. Tsuneda, and K. Hirao, Chem. Phys. Lett. **420**, 391 (2006).
[44] K. N. Walzl, C. F. Koerting, and A. Kuppermann, J. Chem. Phys. **87**, 3796 (1987).
[45] B. Mennucci, R. Cammi, and J. Tomasi, J. Chem. Phys. **109**, 2798 (1998).
[46] N. S. Bayliss and E. G. McRae, J. Phys. Chem. **58**, 1006 (1954).
[47] F. Aquilante, M. Cossi, O. Crescenzi, G. Scalmani, and V. Barone, Mol. Phys. **101**, 1945 (2003).